

## **A population balance approach for the description of water osmosis and intracellular ice formation during cryopreservation**

S. Fadda, A. Cincotti, G. Cao

Dipartimento di Ingegneria Chimica e Materiali, Università degli Studi di Cagliari,  
Piazza d'Armi, 09123 Cagliari, Italy

A novel model capable of quantitatively describing and predicting Intracellular Ice Formation (IIF) as a function of temperature in a cell population during the cooling stage of a cryopreservation protocol, without Cryo-Protective Agent (CPA) is proposed. The model accounts for water osmosis and IIF occurrence during freezing of the cell population, whose size distribution dynamics is simulated by means of a suitable population balance approach. It is found that IIF temperature depends upon the cell size, i.e. it is higher for larger cells. Correspondingly, the Probability of IIF (PIIF) results to be dependent on the initial size distribution of the cell population. Model reliability is successfully verified by predicting experimental data available in the literature of PIIF at different, constant cooling rates with better accuracy as compared to previous theoretical approaches.

### **Introduction**

In the field of tissue engineering, cryopreservation of biological cells represents a current evolving technology where significant advances have been made to date, but several challenges remain (cf. Karlsson and Toner, 2000). Cryopreservation of cells, typically with the presence of CPAs, involves cooling to subzero temperatures, storage, and thawing. During cooling, ice initially forms in the extracellular medium surrounding the cells. As the extracellular ice grows, the extracellular solute concentration increases, thus imposing a chemical potential difference between the cytoplasm and the unfrozen external solution which generates the osmotic transport of water through the plasma membrane. However, if the time scale for the cooling process is short compared to that one for membrane transport, low temperatures are reached before significant dehydration takes place, and thus the cytoplasmic solution becomes supercooled. In such a case, a driving force for IIF is established. Since serious damage and injury occur during freezing when IIF takes place, for successful cryopreservation protocols avoiding IIF is mandatory. In order to help optimization of freezing protocols, several mechanistic models have been developed for predicting the behavior of cells during freezing, along the lines of the pioneering work of Mazur (Mazur, 1963). These models simulate the behaviour of a single, representative (i.e. average) cell during

freezing-thawing processes, while relating the PIIF to the nucleation rate by assuming a sporadic nucleation mechanism (cf. Toner *et al.*, 1992). However, it is difficult to accept on physical grounds that a relatively high number of cells used in a standard cryopreservation protocols are identical, and that identical cells subjected to the same freezing cycle exhibit different temperatures for IIF due to a nucleation process stochastic in nature. Indeed, as already observed in the literature (cf. Mazur 1963), large cells are characterized by smaller surface-to-volume ratio than small ones, and, therefore are expected to loose less water during the cooling stage. Consequently, at any given cooling rate large cells should retain an higher percentage of internal water than small ones, so that at a given temperature a greater supercooled state should be reached. According to this picture, a population of differently sized cells subjected to the same freezing protocol should exhibit different IIF temperatures. On the basis of these considerations, in the present study a novel model which simulates water osmosis along with IIF occurrence during freezing of a cell population characterized by a size distribution is proposed. Specifically, the model couples the classical water transport equation developed by Mazur (1963) to the nucleation and diffusion-limited growth of ice crystals, in the framework of a 1-D PBE which simulates the dynamics of a cell population volumic distribution during the cooling stage of a standard cryopreservation protocol without CPA.

### Model equations

The proposed model simulates the cooling stage of a population of spherical biological cells with a certain size distribution suspended in a water/sodium chloride solution. Each cell is modeled as a semipermeable membrane, as depicted in Figure 1.

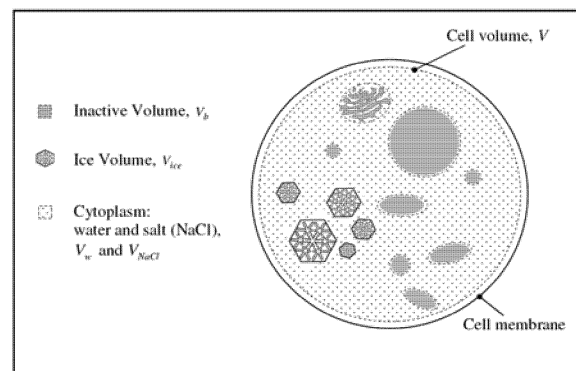


Figure 1 Schematic illustration of the cell model.

Proteins, organelles and other macromolecules are representative of the cell volume  $V_b$  which remains inactive to all physical processes considered in the proposed model. On the other hand, total cell volume  $V$  changes due to exosmosis of water occurring during freezing as well as to intracellular ice crystal nucleation and growth. Water osmosis and IIF are responsible of intracellular salt concentration variations by determining water and ice volumes, i.e.  $V_{water}$  and  $V_{ice}$ , respectively.

The model is based on the following simplifying assumptions:

- Cells are suspended in a solution whose initial conditions are isotonic;
- The extracellular solution is in thermodynamic equilibrium with extracellular ice seeded at a specific temperature,  $T_{seed}$ ;
- Constant densities and negligible difference between ice and liquid water densities;
- Constant osmotically inactive cell volume fraction,  $v_b$ ;
- Negligible impingement between intracellular ice crystals.

Model equations are summarized in Table 1.

Table 1 Model equations.

<b>Cooling temperature dynamics</b>	
$T(t) = T^0 - B \cdot t$ or $\begin{cases} T = T^0 & t = 0 \\ T = T_{seed} & t > 0 \end{cases}$ (1)	
<b>Cell population volumic distribution dynamics</b>	
$\frac{\partial n(V;t)}{\partial t} + \frac{\partial[G_v(V) \cdot n(V;t)]}{\partial V} = 0$ $\begin{cases} n(V;t) = n^0(V) & \text{at } t = 0 : \forall V \in [0, +\infty[ \\ \int_0^{+\infty} n(V;t) dV = N_{tot}^0 & \forall t \end{cases}$ (2)	
<b>Osmotic water transport dynamics</b> $T_e \leq T \leq T_{seed}$	
$\frac{dV}{dt} = G_v(V) = -\frac{L_p(t) \cdot A(t) \cdot \Re \cdot T(t)}{v_{H_2O}} \ln\left(\frac{x_{H_2O}^{int}(t)}{x_{H_2O}^{ext}(t)}\right)$ ; $V = V_0$ at $t = 0$ (3)	
$x_{H_2O}^{int}(t) = \left[ \frac{MW_{H_2O}}{MW_{NaCl}} \left( \frac{S_{NaCl}^{int}(t)}{100 - S_{NaCl}^{int}(t)} \right) + 1 \right]^{-1}$ (4)	
$S_{NaCl}^{int}(t) = \frac{c_0 \cdot V_0 \cdot (1 - v_b) \cdot MW_{NaCl}}{c_0 \cdot V_0 \cdot (1 - v_b) \cdot MW_{NaCl} + \rho_{H_2O} \cdot V_{water}(t)} \times 100$ (5)	
$x_{H_2O}^{ext}(t) = \left[ \frac{MW_{H_2O}}{MW_{NaCl}} \left( \frac{S_{eq}(t)}{100 - S_{eq}(t)} \right) + 1 \right]^{-1}$ (6)	
$T(t) = 273.15 - (0.6) \cdot S_{eq}(t) - (1 \times 10^{-3}) \cdot S_{eq}^2(t) - (4.5 \times 10^{-4}) \cdot S_{eq}^3(t)$ (7)	
$L_p(t) = L_{p,ref} \cdot \exp\left(-\frac{E}{\Re} \left( \frac{1}{T(t)} - \frac{1}{T_{ref}} \right)\right)$ (8)	
$A(t) = 4\pi \cdot \left(\frac{3}{4\pi}\right)^{\frac{2}{3}} \cdot V(t)^{\frac{2}{3}}$ (9)	
<b>Intracellular liquid water volume</b>	
$V_{water}(t) = V(t) - V_b - V_{ice}(t) - V_{NaCl}$ (10)	
$V_b = v_b \cdot V_0$ (11)	
$V_{NaCl} = v_{NaCl} \cdot n_{NaCl} = v_{NaCl} \cdot c_0 \cdot (1 - v_b) \cdot V_0$ (12)	
<b>Intracellular ice mass balance</b>	
$V_{ice}(t) = \begin{cases} 0 & \text{if } N_{ice}(t) = 0 \\ \sum_{i=1}^{N_{ice}(t)} \frac{4\pi}{3} [r_i(t)]^3 & \text{if } N_{ice}(t) \geq 1 \end{cases}$ ; $N_{ice}(t) = \text{int}(\overline{N}_{ice}(t))$ (13)	
<b>Nucleation of ice crystals</b>	<b>Growth of ice crystals</b>
$\frac{d\overline{N}_{ice}}{dt} = B_0(t)$ ; $\overline{N}_{ice} = 0$ at $t = 0$ (14)	$\begin{cases} r_i(t) = 0 & \text{at } t < t_i \text{ when } N_{ice}(t) = 0 \\ \frac{dr_i}{dt} = \overline{D}(t) \cdot \frac{\Omega_g(t)}{r_i} ; r_i(t) = r^*(t) & \text{at } t = t_i \forall i \in [1; N_{ice}(t)] \end{cases}$ (23)
$B_0(t) = J(t) \cdot (V(t) - V_b - V_{ice}(t))$ (15)	
$J(t) = J_0 \cdot D(t) \cdot \exp\left(-\frac{E_N(t)}{k_B \cdot T(t)}\right)$ (16)	
$E_N = \frac{4}{3} \pi \cdot \gamma \cdot r^{*2}$ (17)	$\Omega_g(t) = \frac{x_{H_2O}^{int}(t) - x_{H_2O}^{ext}(t)}{1 - x_{H_2O}^{ext}(t)}$ (24)
$r^*(t) = \frac{2 \cdot \gamma \cdot v_{ice}}{\Re \cdot T(t) \cdot \ln\left(\frac{x_{H_2O}^{int}(t)}{x_{H_2O}^{ext}(t)}\right)}$ (18)	$\overline{D}(t) = \sqrt{D(t) \cdot D_{eq}(t)}$ (25)
$D(t) = \frac{k_B \cdot T(t)}{6\pi \cdot a_0 \cdot \eta(t)}$ (19)	
$\eta(t) = \eta_w(T) \cdot \exp\left(\frac{k_e \cdot \phi_s \left(\frac{S_{NaCl}^{int}(t)}{100 - S_{NaCl}^{int}(t)}\right)}{1 - Q \cdot \phi_s \left(\frac{S_{NaCl}^{int}(t)}{100 - S_{NaCl}^{int}(t)}\right)}\right)$ (20)	<b>Intracellular fractional ice volume distribution</b>
$\phi_s \left(\frac{S_{NaCl}^{int}(t)}{100 - S_{NaCl}^{int}(t)}\right) = \frac{MW_{NaCl}}{\rho_{H_2O}} \left( \frac{100}{S_{NaCl}^{int}(t)} - 1 \right) + v_{NaCl}$ (21)	$\eta_{ice}(t) = \frac{V_{ice}(t)}{V(t) - V_b}$ (26)
$\eta_w(T) = A_w \cdot \left(\frac{T(t)}{225}\right)^\mu$ ; $T > 225 K$ (22)	<b>Probability of Intracellular Ice Formation</b>
	$PHF(t) = \frac{\int_0^{+\infty} n(V;t) \mathbb{1}_{\eta_{ice} \geq 50\%} dV}{N_{tot}^0}$ (27)

Details about model equations are reported in Fadda *et al.* (2009). In the next section, model results will be discussed and analyzed by considering suitable experimental data available in the literature (cf. Toner *et al.*, 1992). Specifically, the temperature at which IIF occurred under given freezing conditions was experimentally determined from the darkening of the cell due to the light scattering from small ice crystals forming inside the cells. The number of iced-up cells was then evaluated using the available cryomicroscopic system. Correspondingly, at each temperature level, PIIF was measured as the fraction of cells (with respect to the total initial ones) cumulatively frozen at that temperature. In order to make an appropriate comparison with these experimental data, in this work it is assumed that cells are iced-up when the ice volume percentage, defined through Equation 26 in Table 1, reaches the value of 0.5. Accordingly, the PIIF is calculated as shown in Equation 27 of Table 1. It is apparent that through this definition, the theoretical PIIF may be safely compared to the corresponding experimental quantity. In fact, while the denominator represents the total number of cells, the numerator displays a cumulative character, thus providing the cells cumulatively “frozen” at the given temperature.

## Results and discussion

The mathematical model proposed in this work (cf. Table 1) is applied to quantitatively describe and predict IIF taking place in a cell population characterised by a size distribution during the cooling stage of a standard cryopreservation protocol where no CPA is used. The proposed model contains a large number of parameters. Many of them may be taken from the literature. Others are specific of the particular cell lineage at hand, or are not available in the literature. Therefore, they are considered as adjustable parameters. In particular, in this work, five of them (i.e.  $L_{p,ref}$ ,  $E$ ,  $v_b$ ,  $J_0$  and  $\gamma$ ) are obtained directly through regression analysis by fitting experimental data in terms of PIIF as a function of temperature. Specifically, the data reported by Toner *et al.* (1992) are considered. These data are related to 60 isolated rat hepatocytes subjected to cryopreservation without CPA, under a cooling rate of  $-400^\circ\text{C}/\text{min}$ . On the basis of the size distribution of this cell population experimentally measured by Toner *et al.* (1992), the initial condition  $n^0(V)$ , necessary for PBE (Eq. 2) integration, has been determined, as reported in Figure 2a. Using this initial cell size distribution, regression analysis has been performed. The comparison between model results and experimental data is shown in Figure 2b, while the obtained values of the adjustable parameters are reported in Table 2. As it can be seen, a good agreement is achieved. Since the aim of this work is to demonstrate that IIF taking place during a standard cryopreservation protocol results to be dependent on the initial size distribution of a cell population, two additional fictitious, narrow, initial cell number density distributions will be also considered, as reported in Figure 2a. It is apparent from Figure 2a that the two fictitious distributions are characterized by mean values which correspond to the smallest and the largest size class cell of the experimental distribution, respectively. These narrow distributions, indeed, have been adopted as initial condition of the proposed model in order to highlight the different behaviour of large and small cells of the experimental distribution shown in Figure 2a. The results of these simulations are both reported in Figure 2b for sake of comparison. As it is apparent, by adopting the two fictitious initial distributions

reported in Figure 2a, while keeping constant all the other parameters and operative conditions of the experimental run, the PIIF vs system temperature simulated by the proposed model is completely different. In particular, the model predicts no IIF down to  $-16\text{ }^{\circ}\text{C}$  for the case of the narrow, small size distribution of the cell population, while an abrupt increase of PIIF takes place around  $-5.5\text{ }^{\circ}\text{C}$ , for the case of the narrow, large sized cell population. Thus, differently sized cells in a population exhibit a different IIF temperature under the same operative conditions. Specifically, the temperature of IIF is higher for the larger cells and, correspondingly, smaller cells are less prone to IIF. The reliability of the proposed model is then tested by predicting the experimental run reported in Figure 3. Here, the fractional cell volume at a constant holding temperature of  $-1.1\text{ }^{\circ}\text{C}$  ( $=T_{seed}$ ) is shown in Figure 3a. Clearly, in the proposed model applied to simulate these experimental data, the temperature initially at ambient value, is changed at  $t > 0$  and kept constant at  $-1.1\text{ }^{\circ}\text{C}$  as reported in Equation 1 of Table 1.

Specifically,  $\int_0^{+\infty} V \cdot n(V;t) dV / \int_0^{+\infty} V \cdot n^0(V) dV$ , representing the average fractional

volume of the cell population characterized by a size distribution as calculated by the proposed model, is compared in Figure 4 with the experimental data taken from literature. It may be seen that a good matching is obtained, thus showing the prediction capability of the proposed model. Additionally, due to the relatively high system temperature, IIF does not really take place during this experimental run, and, accordingly, the proposed model predicts no ice nucleation and growth inside any size class of the cell population. The predictive model capability has been further tested by comparing experimental data with model results in terms of PIIF at  $-40\text{ }^{\circ}\text{C}$  as a function of the cooling rate. The cumulative fractional number of cells that undergo IIF at  $-40\text{ }^{\circ}\text{C}$  reported in Figure 3b is predicted with a reasonable accuracy when the cell size distribution experimentally determined, and reported in Figure 2a, is adopted. The matching is definitely better than the one obtained by the model proposed by Toner *et al.* (1992), also reported in figure 3b, where a sporadic nucleation in a population of identically sized cells is assumed.

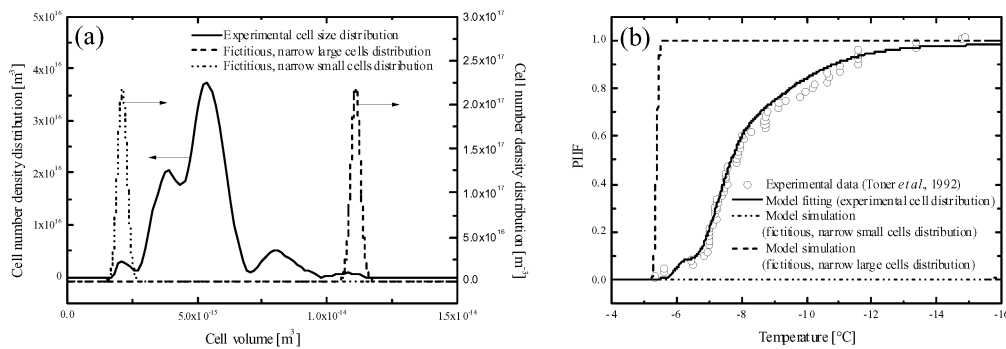


Figure 2 Cell number density distributions as a function of cell volume used as initial condition for PBE model(a), and comparison between experimental data and model results in terms of PIIF for a population of rat hepatocytes cooled at  $-400\text{ }^{\circ}\text{C}/\text{min}$  (b).

Table 2 Adjustable model parameters.

Parameter	value	unit
$E$	$2.66 \times 10^5$	$[J \text{ mol}^{-1}]$
$J_0$	$2.1 \times 10^{24}$	$[\# \text{ m}^{-3}]$
$L_{p,ref}$	$8.89 \times 10^{-13}$	$[m^3 \text{ N}^{-1} \text{ s}^{-1}]$
$v_b$	0.465	$[-]$
$\gamma$	$1.148 \times 10^{-3}$	$[J \text{ m}^{-2}]$

In particular, a vertical, abrupt increment of  $PIIF|_{-40^\circ\text{C}}$  at about  $-100^\circ\text{C}/\text{min}$  is predicted by Toner *et al.* (1992). Interestingly, this behaviour could be obtained by the model here proposed if a population of identically sized cells was taken into account. The global picture is that, small and large cells in a population of the same lineage may behave quite differently, being the larger ones able to form internal, lethal ice much easier. Therefore, post-thaw viability of a cell population characterized by a relatively wide size distribution may result positive for the small cells initially present, since the selective IIF has preferentially killed large cells. Consequently, optimization of a standard cryopreservation protocol in general needs to take into account the naturally present, relatively wide size distribution inside any cell population.

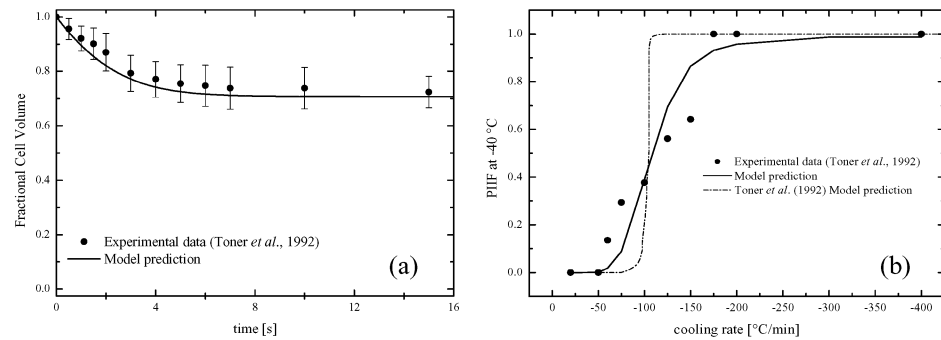


Figure 3 Comparison between experimental data and model prediction in terms of temporal behaviour of the average fractional cell volume at a constant holding temperature of  $-1.1^\circ\text{C}$  (a), and in terms of  $PIIF$  at  $-40^\circ\text{C}$  as a function of cooling rate.

## References

- Fadda S., A. Cincotti, G.Cao. The effect of cell size distribution during the cooling stage of cryoconservation without CPA.2009; Manuscript in preparation.
- Karlsson JOM, Toner, M. Cryopreservation. In: Lanza R, Langer R, Vacanti J. Principles of Tissue Engineering (Second edition). Academic press, Inc., 2000: 293-306.
- Mazur P. Kinetics of water loss from cells at subzero temperatures and likelihood of intracellular freezing. J Gen Physiol.1963; 47: 347-369.
- Toner M, Tompkins RG, Cravalho EG, Yarmush ML. Transport phenomena during freezing of isolated hepatocytes. AIChE J. 1992; 38: 1512-1522.